EFFECT OF THE VORTEX SPRINGING FROM A HELICOPTER BLADE TIP ON THE FLOW AROUND THE NEXT BLADE

BY
Bernard Monnerie and Alain Tognet

Translation of "Influence du Tourbillon Marginal Issu D'Une Pale D'Helicoptere sur L'Ecoulement Autour de la Pale Suivante", ~~Extrait de~~ l'Aeronautique et l'Astronqutique, No. 29, 1971-5, pp 24-32

NATIONAL AERONAUTICS AND SPACE ADMINISTRATION
WASHINGTON, D.C. 20546 FEBRUARY 1972

(for this reason the study was financially supported by the rotary wing section of the S. T. Aé.). Meanwhile, the study is sufficiently broad in nature and the applications go beyond the framework of helicopters. It concerns, in effect, a fundamental study of the vortexes springing from the wings of limited airfoil span and from the action that these can have on the aerodynamics of the carrying surfaces located in their proximity.

The problem, for example, concerns the empennages and the tail fins of planes which are almost always placed in the aerodynamic field markedly affected by the wing and the vortexes which the wing emits.

For helicopters, as a result of the rotation and the number of blades, the vortexes affect the aerodynamics of the blades themselves.

The photograph shown in Plate 1 provides a view of the hydrodynamic tunnel /1/ in which the vortex of a rotor for an advancement parameter of 0.3 is shown. One sees in particular that the vortex springing from blade No. 3 passes close to blade No. 1 and as a result affects its behavior.

In a systematic fashion, Plate 2 presents the blade positions for various vortexes encountered in the course of one revolution of a three-bladed helicopter having a parameter of advancement of 0.3.

Among all these configurations, two cases are particularly interesting because they lend themselves both to experimental analysis and to theoretical analysis. It concerns cases where the vortex is either perpendicular or parallel to the blade.

The proposal here is to study the perpendicular vortex effect

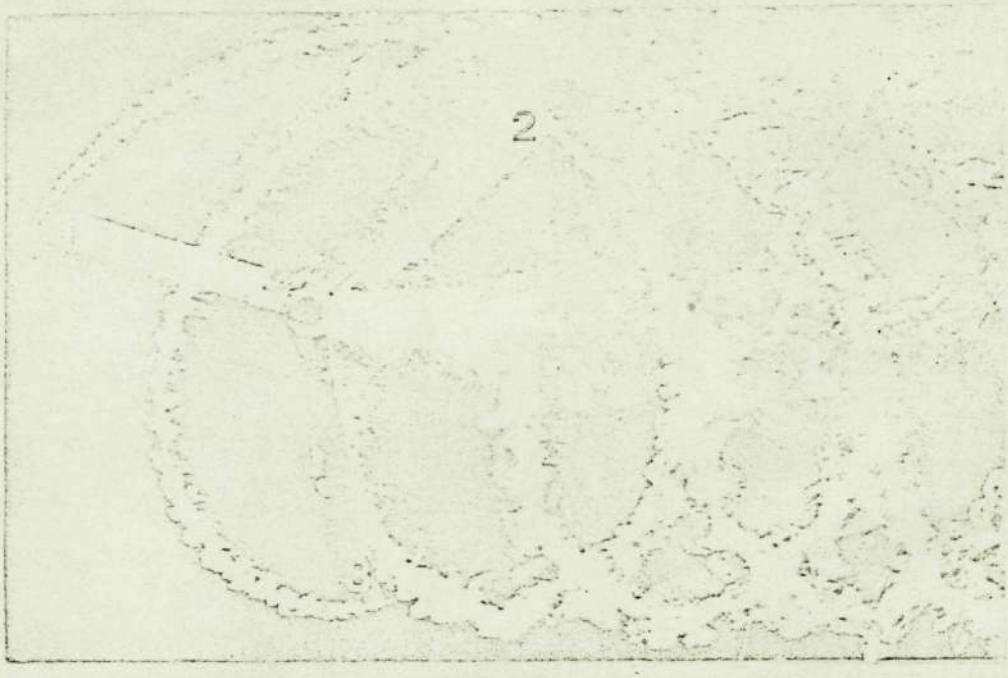

Plate 1 - View of the vortex in the hydrodynamic tunnel.

$$\mu = \frac{V_o}{\Omega R} = 0{,}3$$

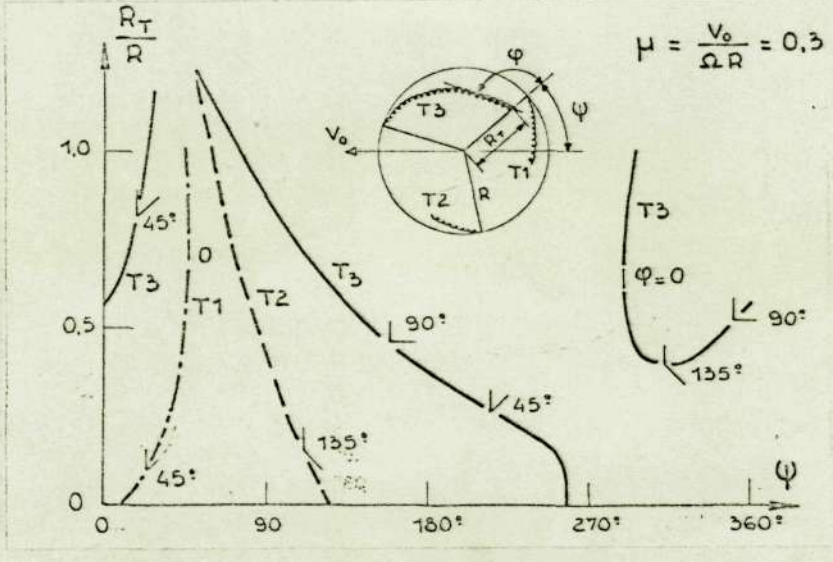

Plate 2 - Intersections of the vertical plane of blade 1 with the various vortexes. (Three-bladed rotor)

$$(\mu = \frac{V_o}{\Omega R} = 0{,}3)$$

on the airfoil span of the blade to determine how performance is affected and which parameters control the phenomenon.

To that end, the structure of vortexes will be analyzed, which will provide a composite of results useful for later studies dealing with helicopter noise. There are, as a matter of fact, indications from experiments (Plate 3) which show that the shape of the blade tip can have a significant affect on helicopter noise [2, 3].

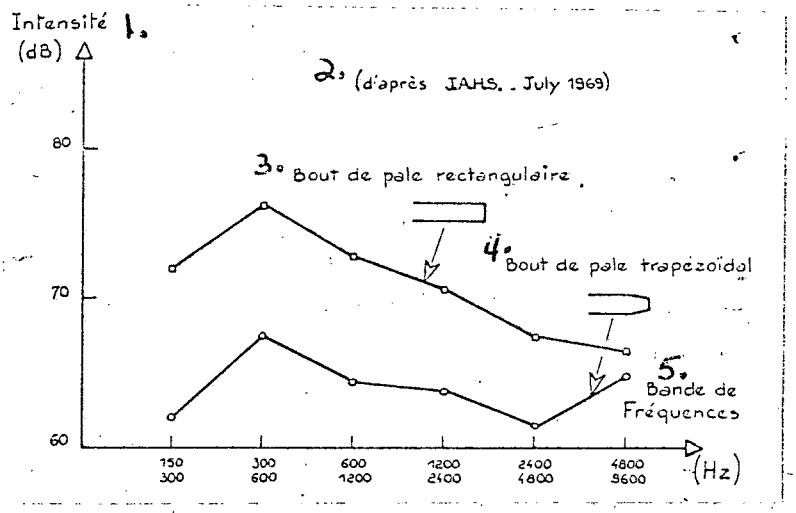

Key:
1. Intensity
2. (According to J.A.H.S. July 1969)
3. Rectangular blade tip
4. Trapezoidal blade tip
5. Frequency band

Plate 3 - Influence of the shape of the blade tip on noise.

The account which follows will be the focal point of this study undertaken in 1969, and whose initial results were presented to the AFITAE Congress of Applied Aerodynamics of 1969.* It will consist of five parts:

1 - Effects of a vortex on load distribution and overall forces.

2 - Influence of the shape of the blade tip which created the vortex.

*Unpublished report of Ph. Poisson-Quinton.

3 - Tests of the vortex.

4 - Elaboration of a method of computing induced loads. Comparison with experiments.

5 - Computation of the rolling-up effect of the vortex.

1. Effect of a Vortex in the Upstream Flow of a Blade

1.1. Setup (See Plate 4)

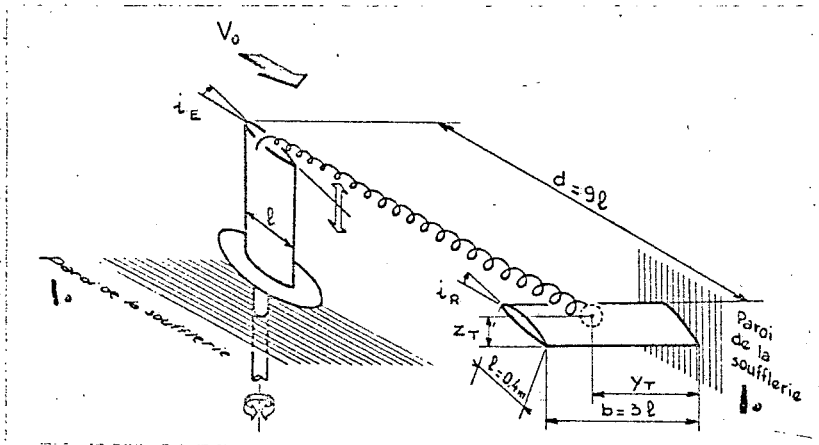

Key:
1. Wall of the wind tunnel
2. And

Plate 4 - Simulation of the effect of the vortex of a blade on the next blade. $y_T/b = 0,4$ et $0,8$ $-0,5 < z_{T/l} < 1$

The test model consists of a piece of helicopter blade with a length of $4b^2/S = 6$, an airfoil span of 1.2 m (b), and a chord of 0.4 m (l). The test model is mounted horizontally and balanced on the wall of the wind-tunnel. The model has orifices used to measure pressures in 8 sections (profile NACA 0012). This blade, on which an upstream vortex will be allowed to react, is termed the receptor blade and is designated by the index R.

A second model termed the emitter blade (index E), which has the same general characteristics as the first, is placed vertically

in the convergence of the wind tunnel* at a distance of approximately 9 chords from the receptor blade. The model is on a plate whose altitude can be regulated to set the altitude of the vortex with respect to the receptor wing. The tip of this model is convertible, which permits the shape of the blade tip to be changed.

We will show the differences between the aerodynamic characteristics of the blade with and without a vortex in the incidence of flow. It must be stated that this configuration only appears simple. The configuration corresponds to one in a limitless atmosphere which is much more complicated and which consists of numerous vortexes: the principal vortex and the vortex at the foot of the blade and their images in relation to the wall of the wind tunnel.

1.2. Effect on Pressures

The presence of the vortex modifies the local incidence of the various sections of the blade. When the incidence of the vortex has the same direction as the vortex emitted by the receptor blade (i_E and i_R of the same sign), the absolute value of the local incidence is increased by the vortex for the sections between the blade tip and the projection of the vortex on the blade; the value is diminished by the others.

On Plate 5 is shown the evolution of the distribution of pressures for two sections framing the vortex.

---

*The tests were made in the Cannes wind tunnel. All the results of measurements are provided in a series of unpublished test records.

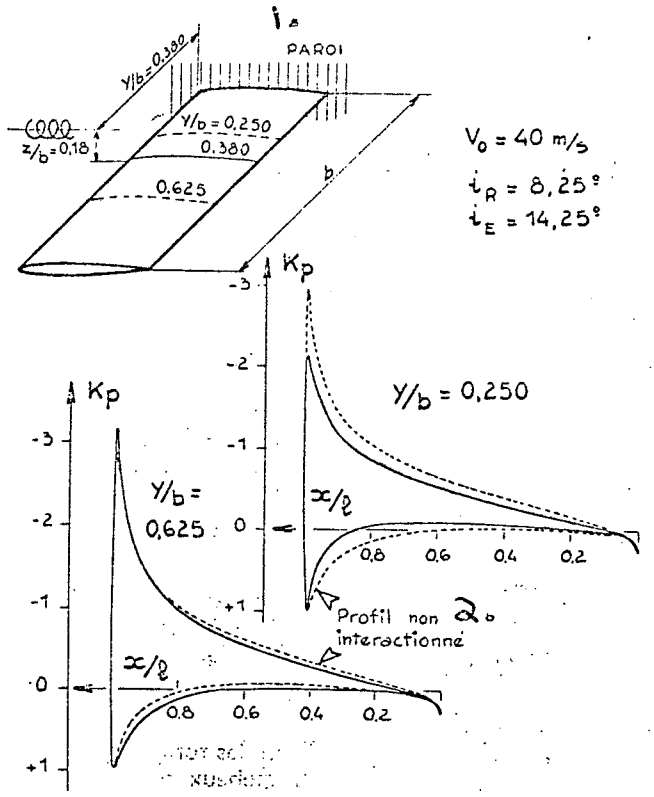

Key:

1. Wall
2. Non-interacted profile

Plate 5 - Influence of the vortex on pressure distribution.

1.3. Effect on the Overall Forces

Plate 6 shows the variation of overall forces which take place as a result of the vortex. The curve $C_z = f(i)$ experienced a translation corresponding to a reduction of the average incidence of approximately 2 degrees for this configuration. The pole is deformed, and a very sensitive increase is recorded of the C_x associated with a given C_z; for example, for $C_z = 0.6$ $\Delta C_x/C_x = +67\%$

1.4. Influence of the Position

The results given in paragraphs 1.2 and 1.3 are a function of

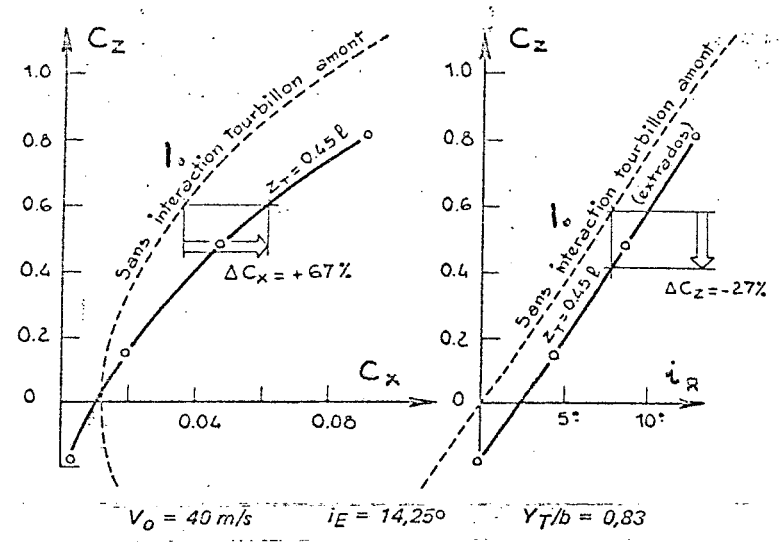

Key:

1. Without interaction of upstream vortex

Plate 6 - Effects of the interaction on overall forces.

the position and of the intensity of the incidence of the vortex.

Plate 7 shows the evolution of the variation of the lifting capacity ΔC_z as a function of the altitude of the vortex for two airfoil span positions. The asymmetry observed for the positive and negative z_T comes from the vortex at the foot of the blade.

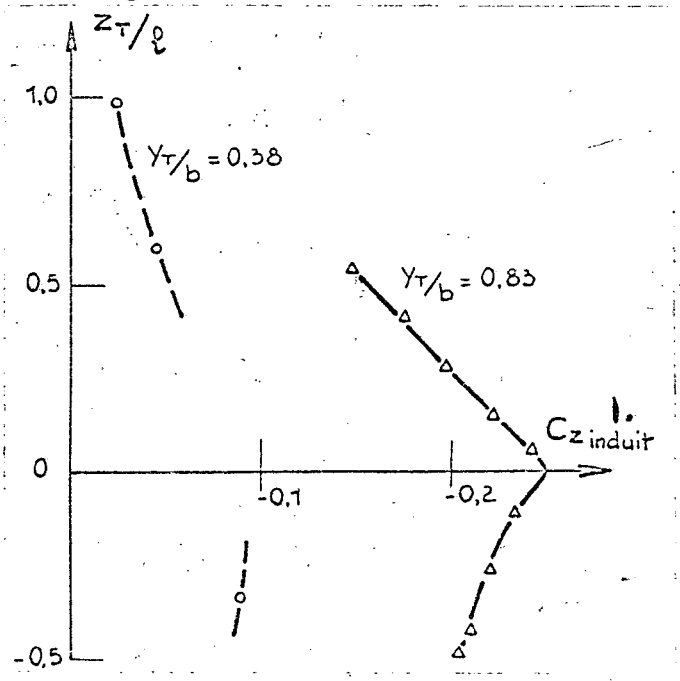

Key:

1. Induced

Plate 7 - Influence of the position of the vortex on the overall forces.

The influence of the airfoil span position is very sensitive. The effect is maximal for a position of the vortex next to the blade tip; it tends to be in the neighborhood of zero when the vortex displaces itself towards the socket.

As far as the influence of the intensity of the vortex of incidence is concerned, it was determined that the effect is a crossing function of the intensity of the perturbation represented by the vortex; the ΔC_z are, for example, proportionate to the incidence, and, therefore, to the lifting capacity of the emitter blade (see Plate 9).

2. Influence of the Shape of the Blade Tip

2.1. Generalities

One of the goals of the experiment was to examine the influence of the various parameters controlling the phenomenon. Among these, it was thought that the shape of the emitter blade tip would be the determining factor.

A large variety of shapes were tried. Plate 8a presents the most interesting: rectangular tip (R+S), parabolic (A and B), trapezoidal (T).

2.2. Results

For all the shapes of blades tested, the variations of the overall forces of the emitter blade are identical when the engendered vortexes occupy approximately the same position with respect to the receptor blade. That is what was established, for example, for the

ΔC_z shown in Plate 9.

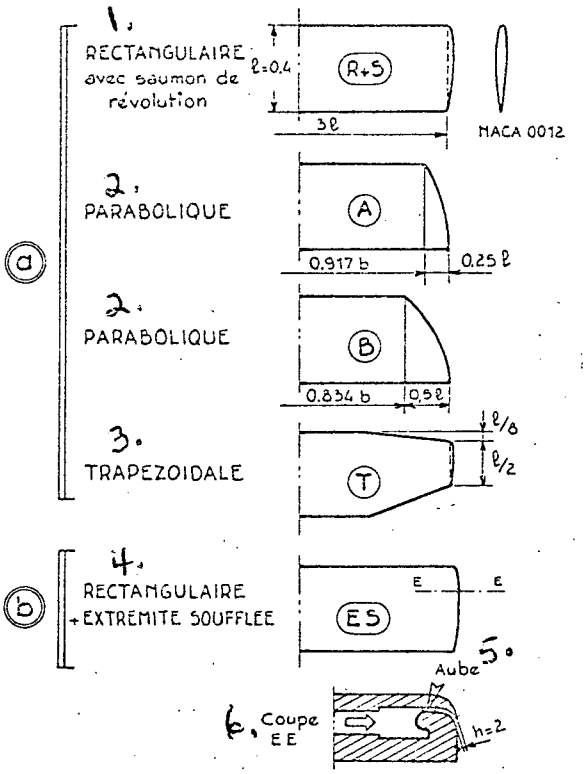

Key:

1. Rectangular
2. Parabolic
3. Trapezoidal
4. Rectangular +thickened tip
5. Blade
6. Section EE

Plate 8 - Blade type. Shape of blade tip.

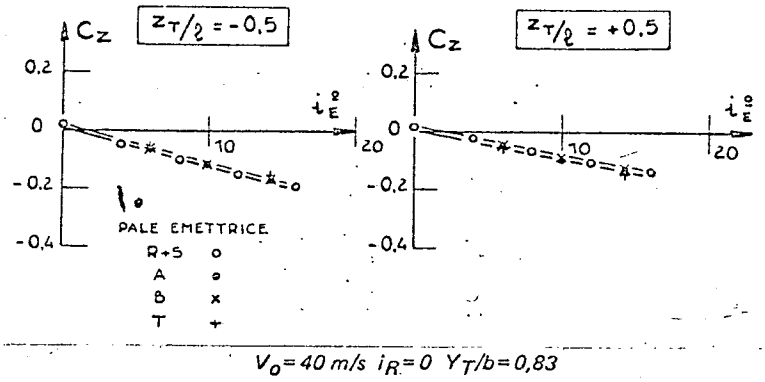

Key:

1. Emitter blade

Plate 9 - Influence of the shape of the emitter blade on the induced C_z.

Such is not the case for the pressures, especially when the vortex is close to the wing; however, the differences observed for the sections closest to the vortex are very sensitive to a variation of the distance between the vortex and this section. Significant comparisons can only be effectuated when the positions occupied by the vortexes are in every respect identical, which is not quite the case for Plate 10. New tests in which the position of the vortex would be marked with great precision would yield more valuable information concerning this aspect.

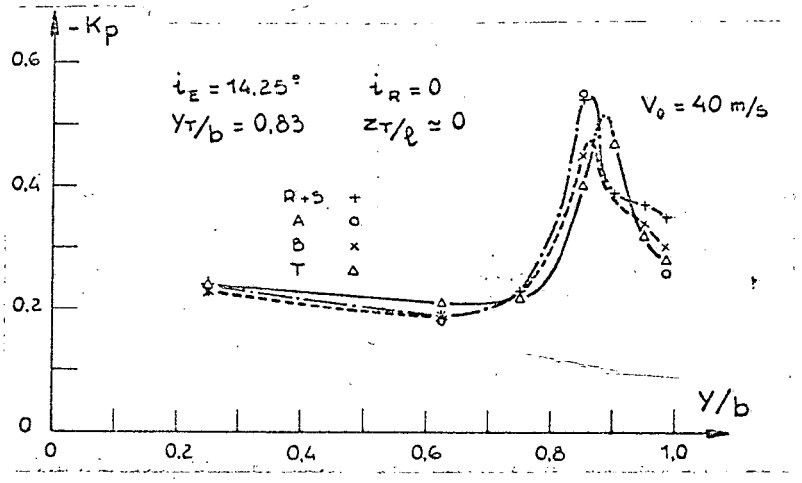

Plate 10 - Effect of the vortex springing from blades R+S, A, B, T on the distribution of pressures on the airfoil span (close to the master coupler).

2.3. Blade with Thickened Tip

In order to modify the organization of the vortex radically, a blade with thickened tip was used (see Plate 8b). In effect, as one will see later, the vortex is significantly altered by the thickening: the trajectory and the distribution of speeds in the center of the vortex are modified.

Nevertheless, it was also determined that for a like position of the vortex the effect on the overall forces is identical to the one noted when the nonthickened emitter blade was placed at the same incidence.

For the modifications of the local pressures, the same assertion made in paragraph 2.2 must be made; a series of special experiments will have to be made to show meaningful differences.

3. Tests of the Vortex

In order to characterize the vortexes which escape from different blade tips and also, in particular, to understand the lessening of perceived noise for a rotor equipped with trapezoidal blade tips, speed measurements were effectuated for the various vortexes.

An anemoclinometric Gruson antenna of 8 mm in diameter, shown in Plate 11, was used.

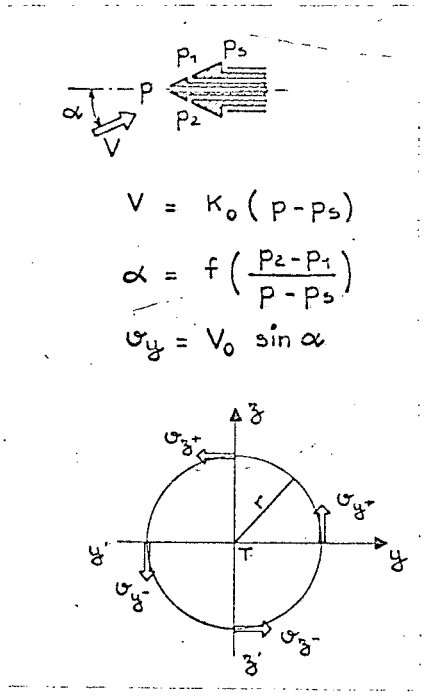

Plate 11 - Clinometric measurements.

Thanks to a preliminary calibration, the orientation and modulus of the speed vector of the measurement of 3 different pressures were determined; $\Delta p_z = p_1 - p_2$, $\Delta p_y = p_3 - p_4$, and $\Delta p_q = p - p_s$. The tests were conducted along horizontal and vertical lines perpendicular to the vortex axis. In these cases, one or the other of the differences Δp_y and Δp_z is null and the analysis is made easy.

The components of the perpendicular speed V_o that were deduced from the measurements of various vortexes are compared in Plate 12. It was determined that the speeds in vortexes were somewhat lowered by using a trapezoidal blade, and that speeds were considerably lower when using a blade with a thickened tip.

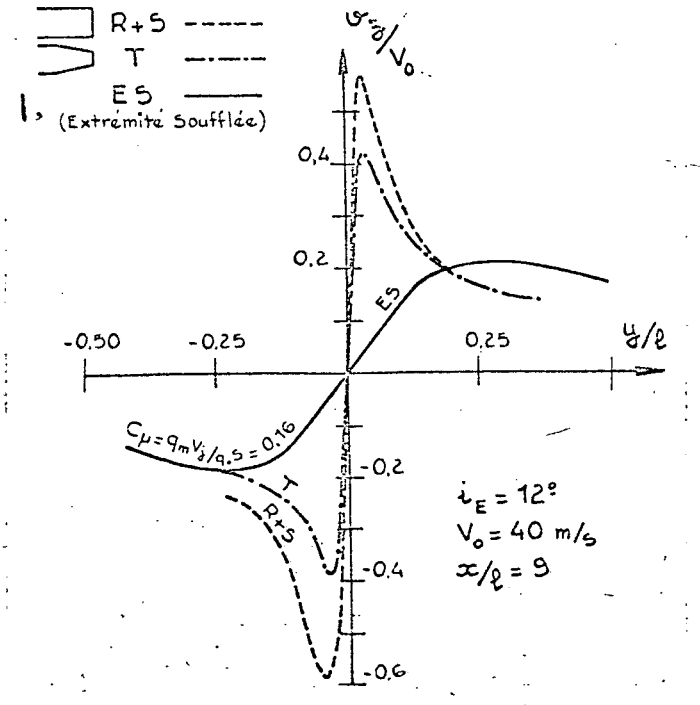

Key:

1. Thickened tip

Plate 12 - Measurements of speeds in the vortexes emitted by the blades "R+S," "T," "E.S."

The distribution of transverse speeds can be managed, in terms of circulation, by hypothesizing that the field of speeds in such a vortex consists of rotation around the vortex axis. This hypothesis is reasonable because the transverse speed curves measured on $z'T_Z$ and $y'T_y$ are somewhat symmetrical with respect to the source and are identical among each other. Under these conditions, the circulation $\Gamma(r)$ of the speed the length of a radius r which has the vortex as its axis will differ little from

$$2\pi r \times \frac{1}{4}(v_{z+} + v_{z-} + v_{y+} + v_{y-})$$

In order to regroup the results corresponding to several speeds and to several incidences of the emitter blade, the circulation $\Gamma(r/l)$ was brought back up to the maximum circulation distribution on the airfoil span along the full length of the blade. This maximum, in our case, corresponds to the socket section.

$$\Gamma_{max} = \frac{1}{2} C_z \text{ socket} \times V_0 \times l$$

The regroupment was aided by the idea that the vortex comes from the rolling up of elementary vortexes, conceived by Pradtl, whose sum total of intensities is Γmax. The regroupment effectuated in this manner (Plate 13) is absolutely satisfactory, considering the degree of precision that one may expect of clinometric measurements made in a vortex.

The curves $\Gamma = f(r/l)$ corresponding to blades which have rectangular, trapezoidal, and thickened tips (shown in Plate 14) confirm the results of Plate 13: the most concentrated vortex corresponds to the

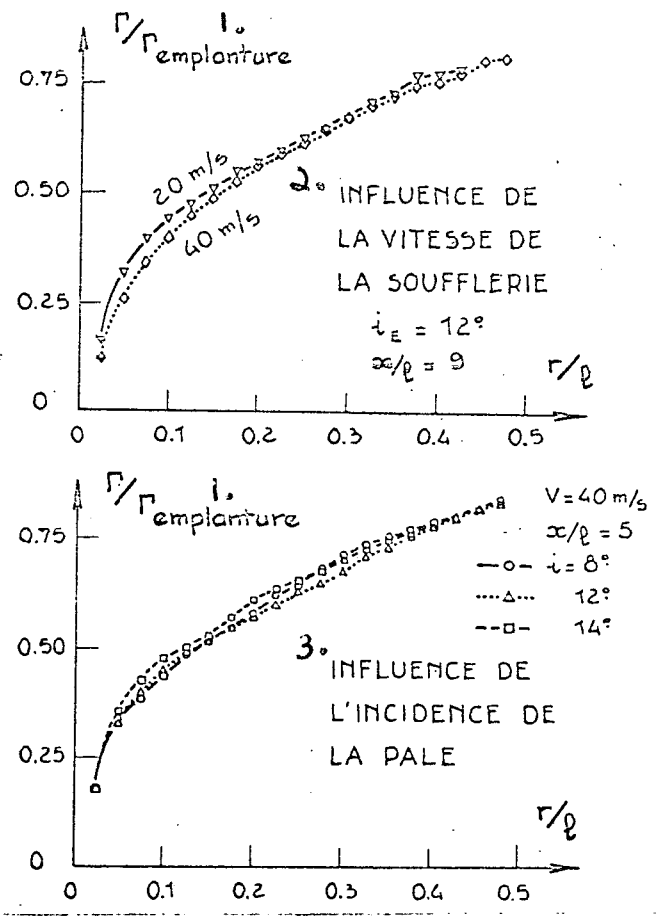

Key:

1. Socket
2. INFLUENCE OF THE SPEED OF THE WIND TUNNEL
3. INFLUENCE OF THE INCIDENCE OF THE BLADE

Plate 13 - Measurement of the circulation in the vortex springing from the blade "T."

rectangular blade; the blade with the thickened tip provided a more diluted vortex.

4. Elaboration of a Computation Method of the Loads Induced by a Vortex on a Wing

We are going to apply the lift line theory to a flow incidence bearing a vortex intensity of Γ_T.

The circulation around a section of wing follows the equation

$$(1)\quad \Gamma(Y) = \frac{1}{2} V_0 l K \left[i - \frac{\omega(Y)}{V_0} \right]$$

ω being the vertical speed induced at the ordinate Y by the vortexes with the intensity $d\Gamma$ distributed all along the airfoil span of the wing and by the vortex ΓT.

$$(2)\quad \omega(Y) = \frac{1}{4\pi} \int \frac{(d\Gamma/dY')\, dY'}{Y - Y'} + \frac{\Gamma_T}{2\pi} \frac{Y - Y_T}{(Y - Y_T)^2 + Z_T^2}$$

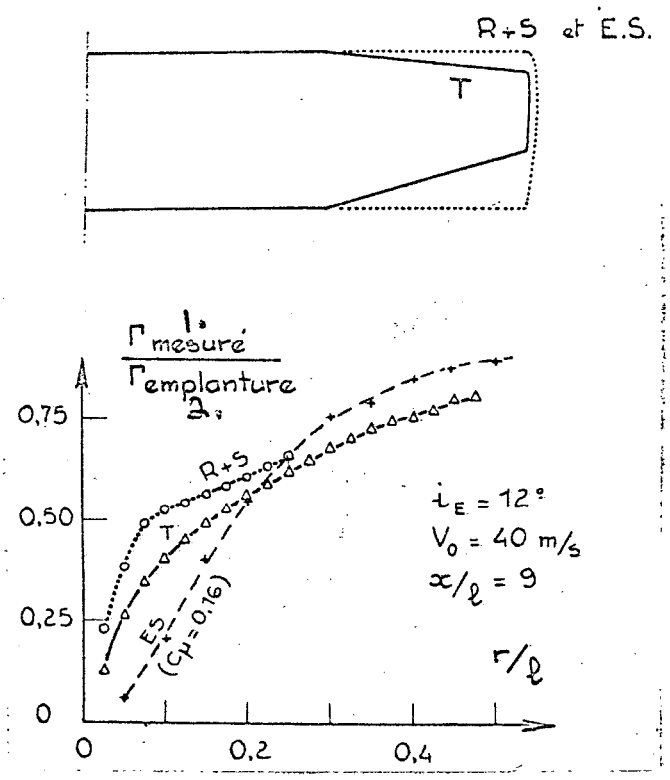

Key:
1. Measured
2. Socket

Plate 14 - Comparison of the circulation distributions in the vortex springing from the blades "R+S," "T," and "E.S."

In the same manner as stated by Simmons /4/, the integro-differential equation which results from (1) and (2) is resolved by replacing the integral by a sum corresponding to a finite number of vortexes. For this, the wing is divided into N intervals YiYi+1 in the middle of which are placed the vortexes with the intensity

$\Gamma(Yi+1) - \Gamma(Yi)$. In writing the equation resulting in each blade tip interval, one obtains a linear system of N - 1 equations to N - 1 unknowns.

The results presented in Plate 15 correspond to a computation effectuated for $\frac{1}{2}$ a blade mounted on the wall in the presence of two vortexes with opposite intensities at a distance from b $\simeq$ 1.2 m (vortex T_M and vortex at the foot of the blade T_{pp}). This computation takes into account the corrections caused by the walls of the wind tunnel. It is determined that the computation represents relatively well the experimentally observed evolution. In effectuating the integration along the airfoil span, one obtains the lifting capacity of the blade in the presence of the vortex, and, therefore, the ΔC_z. Plate 16 compares the results of the computations made during experiments.

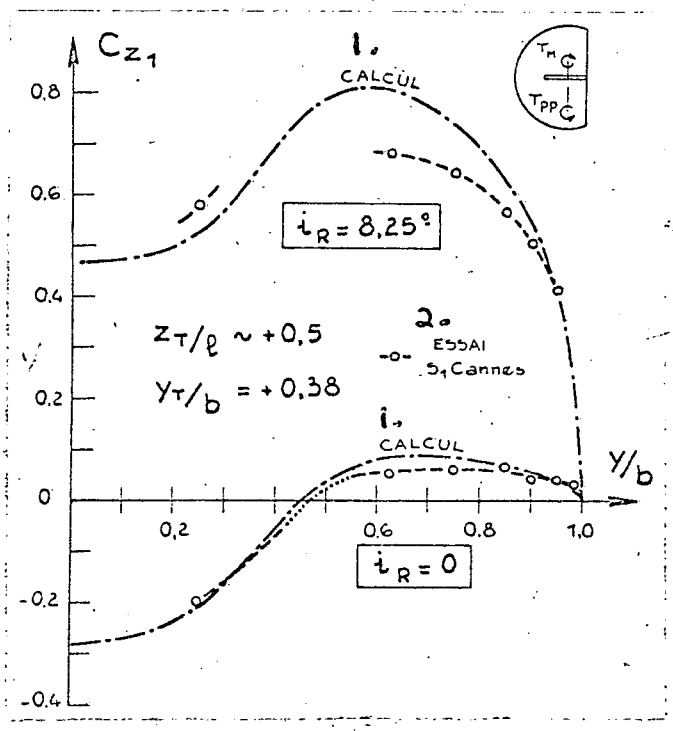

Key:

1. Computation
2. Test S_1 Cannes

Plate 15 - Influence of the vortex on load distributions.

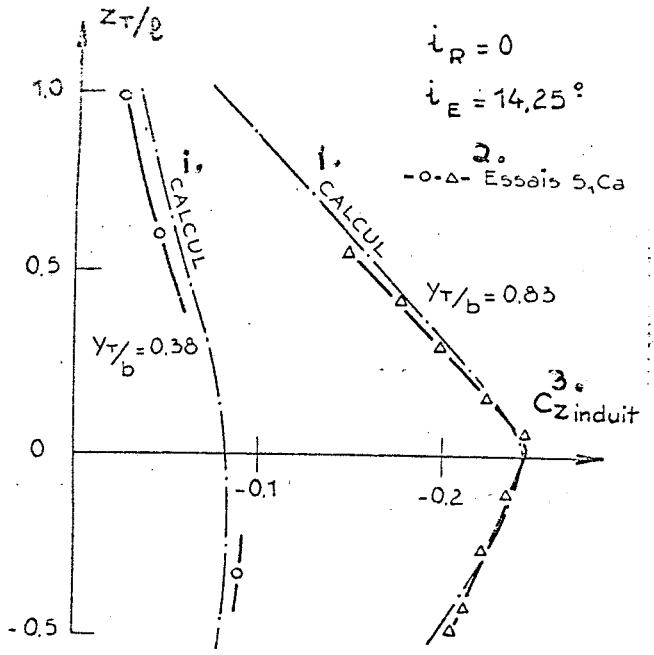

Key:

1. Computation
2. Test S_1 Cannes
3. C_z induced

Plate 16 - Influence of the position of the vortex on overall forces. Comparison of computations and experiments.

5. Computation of the Rolling up of the Vortex

The program brought into focus for the preceding computation provided accessorily, in making $\Gamma T \equiv 0$, the distribution of loads on the airfoil span $\Gamma(Yi)$ for wings no matter what their shape, and as a result a vortex surface which escapes from these wings by discrete vortexes $\Gamma(Yi+1) - \Gamma(Yi)$ located at the points $\frac{Yi+1+Yi}{2}$.

It is possible to compute the induced speed for each vortex by the sum of the others. Therefore, by integrating during a time dt, one obtains the displacement that each vortex experiences as a result of the action of the other vortexes. The new shape of the vortex surface obtained corresponds to an abscissa which has increased by V_o dt.

Such a computation, proposed since 1935 by Westwater [5], overlooks the longitudinal effects of the vortexes which become deformed; however, this approximation is justified and the results obtained are satisfactory.

Plate 17 shows the evolution of sections of the vortex surface coming from a blade with a trapezoidal tip. The rolling-up phenomenon is very well described by the adopted schematization.

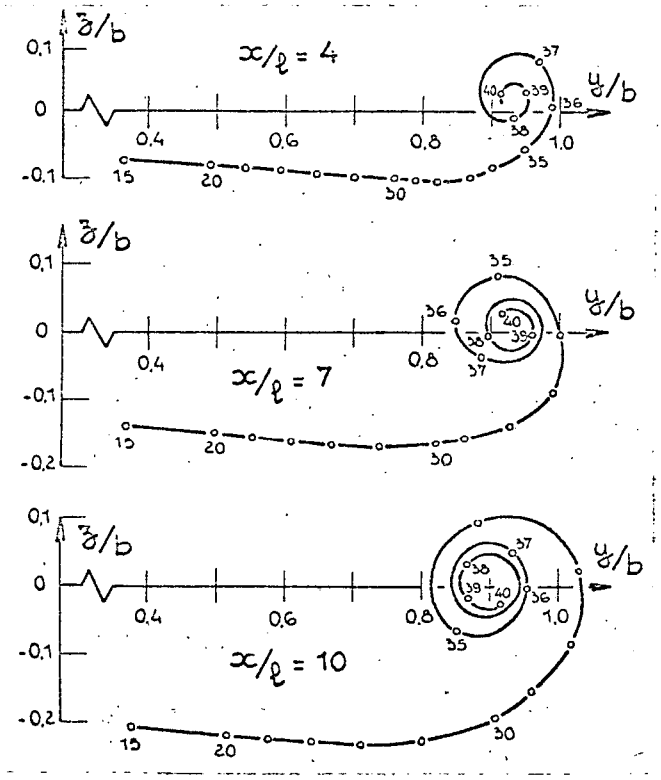

Plate 17 - Rolling up of the vortex surface downstream of a wing with an incidence - i = 10°.

One can determine for each section the approximate trace of the vortex axis (Y_T, Z_T), and from there to obtain the circulation distribution in the vortex $\Gamma(r) = \Sigma\Gamma_j$ for all the j, such that

$$(Y_j - Y_T)^2 + (Z_j - Z_T)^2 < r^2.$$

The curves obtained as a result of computations made with distances of 4.7 and 8.5 chords from the trailing edge are compared in Plate 18 to the results of measurements (see paragraph 3). The determination is made that the curves $\Gamma(r)$ evolve very little as a function of the abscissa for the computation as well as for the experiment, and that the agreement between computation and experiment is good.

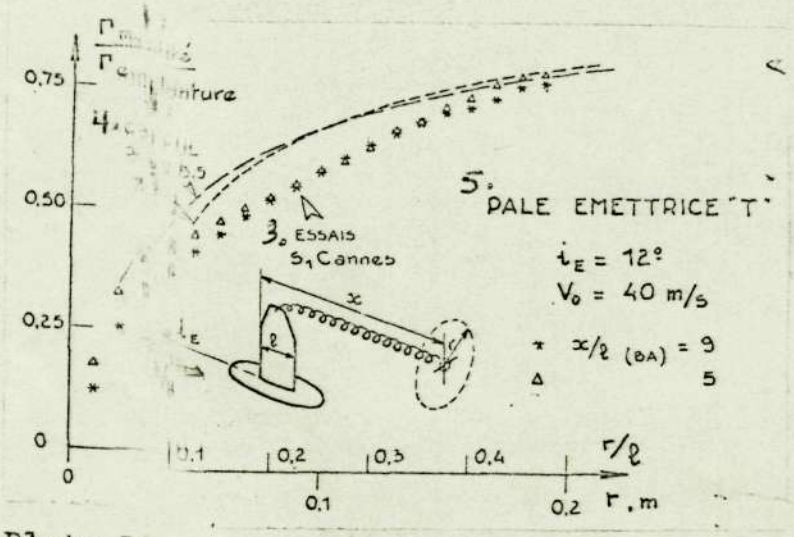

Key:

1. Measured
2. Socket
3. Test S_1 Cannes
4. Computation
5. Emitter blade "T"

Plate 18 - Measurements of the circulation in the vortex - Comparison of the computation and experiment.

6. Conclusions

The effect of a vortex whose axis is parallel to the upstream speed in the flow which surrounds a blade was subjected to experimental study in the wind tunnel S_1 of Cannes and by computation. The rolling up of the vortex surface was computed for several distances x/l behind the emitter blade. It was determined that the resulting circulation distribution varies little beyond x/l = 5, and that it agreed well with the distribution measured in the vortex in the course

of clinometric tests.

The modification of the overall forces resulting from the vortex does not depend on the shape of the emitter blade tip if the vortex is positioned in the same place relative to the receptor blade.

Meanwhile, considering the differences observed for the overspeeds of the vortex, it is probable that the pressure field may be influenced by the geometry of the emitter blade when the vortex is close to the receptor blade. That may be one of the reasons why a reduction of helicopter noise was noticed when the shape of the blade tip was modified.

References

[1] H. WERLE et C. ARMAND. *Mesures et visualisations instationnaires sur les rotors. Communication au Congrès d'Aérodynamique appliquée.* AFITAE 1969. T.P. O.N.E.R.A. nº 777.

[2] R.L. SCHEGEL, W.E. BAUSCH. *Helicopter Rotor Noise Prediction and Control.* J.A.H.S. (July 69).

[3] C.R. COX. *Helicopter Noise Reduction and Its Effects on Operations.* J.A.H.S. (January 1970).

[4] A. SIMMONS. *Some aspects of blade vortex interaction on helicopter rotors in forward flight.* JOURNAL of SOUND and VIBRATION. Vol. 4 number 3 (1966).

[5] F.L. WESTWATER. *Rolling up of the surface of discontinuity behind an aerofoil of finite span.* Aeronautical Research Council Reports and Memoranda nº 1692 (1935).